

A Hopf bifurcation with a strong incommensurate frequency response in quantum wells

Adriano A. Batista¹, Bjorn Birnir² and Pablo I. Tamborenea³

¹*Department of Physics, University of California, Santa Barbara, CA 93106*

²*Mathematics Department, University of California, Santa Barbara, CA 93106*

and Science Institute, University of Iceland, 107 Reykjavik, Iceland

³*Departamento de Física, FCEN, Universidad de Buenos Aires, (1428) Buenos Aires, Argentina*

(November 16, 2018)

The behavior of delta-doped wide quantum well heterostructures in the presence of intense far-infrared radiation is studied using semiconductor Bloch equations. A quantum well is designed where one can either obtain a strong subharmonic (period-doubling) or a strong incommensurate (Hopf) frequency response by varying the sheet density and field strength. These strong responses are easily attainable with current quantum well technology and the field amplitudes and frequencies of the drive are well within the range of the free electron laser.

The effective description of some quantum mechanical systems, far from a classical correspondence, can be nonlinear. Strongly driven THz intersubband transitions in AlGaAs/GaAs quantum wells are a good example of such a system and have been shown to exhibit novel nonlinear phenomena. Many-body effects which cause the nonlinearities become much more prominent in wide quantum wells ($\approx 300\text{\AA}$) where intersubband spacing is of the order of 10meV which is approximately of the order of the electron-electron Coulomb interactions. The main signature of the nonlinearities is the dynamic shielding by the electron gas of the incoming radiation. The screening blue shifts the absorption peak frequency, by an amount proportional to the intersubband population difference and sheet density, to the dressed frequency at which collective oscillations of the entire electron gas occur. This depolarization shift also causes the generation of second-harmonics of the drive frequency when it is at half of this dressed frequency [1]. The depolarization shift and superharmonic generation have been accurately simulated and measured, see [2,1,3]. In addition to this dressing of the intersubband frequency there is a dynamic Stark effect which shifts the absorption peak by an amount proportional to the intensity of the incoming radiation. Experiments by Heyman et al. [1] and Craig et al. [4] showed the intersubband absorption peak distorting and shifting to the red towards the bare intersubband frequency as it saturates with increasing THz intensity. These results were in good agreement with a two-subband density matrix model proposed by Zalužny [5,6].

A superharmonic generation is a general feature of classical nonlinear systems with periodic driving, whereas a subharmonic generation or an incommensurate frequency response are not as ubiquitous and usually require the fine tuning of parameters. The same could be the case in

(effectively nonlinear) quantum mechanical systems and this necessitates a theoretical search for the appropriate parameter ranges. The generic bifurcation from a stationary solution or a fixed point, corresponding to a periodic orbit, in a classical system is a Hopf bifurcation [7] and it typically leads to a response comparable in magnitude to the drive. This motivates the search for a strong response (a Hopf bifurcation from a fixed point) in our effectively nonlinear quantum mechanical system that is a second frequency response of the collective electron excitations incommensurate with the frequency of the laser drive. Theoretically this response can be explained by a parametric oscillation of the electron gas where the system is able to respond at a new frequency that is a dressing (as explained above) of the frequency $E_1 - E_0 = E_{10}$ [8].

Another objective of this letter is to verify the predictions of the model of Galdrikian and Birnir [2] for period doubling bifurcation for a more realistic situation in the quantum well. The present model is more complete and makes less approximations on the electron-electron Coulomb interaction and also includes the exchange terms in the Hamiltonian. On the other hand analytical calculations as the averaging technique used in [9] are considerably more difficult to perform now. Therefore we are limited to focus on numerical results for the nonlinear dynamics.

Sherwin et al. [10,11] have studied the optical properties of wide quantum wells of $Al_{0.3}Ga_{0.7}As$ (barrier) and GaAs (well) driven by the far infrared radiation of the free electron laser (FEL) at UCSB. The epitaxially grown structures are filled with a sheet density of $\approx 1.5 \times 10^{11} e/cm^2$ provided by silicon donor layers located outside of the well. The donors are usually at hundreds of \AA 's away to avoid scattering of the electrons by the dopants, thus increasing the coherent radiation output of the electrons collective oscillations.

Many-body effects on intersubband transitions and optical properties of QWs have been studied mainly with Hartree-Fock and rotating wave approximations for the response of two-(sub)band QWs [12–14]. Based on similar methods Nikonov, Imamoglu et al. [15,16] demonstrated that the influence of exchange and depolarization terms on the absorption or gain spectrum disappears in the limit of very narrow quantum wells. Numerical inte-

gration of the multisubband semiconductor Bloch equations were performed by Tsang et al [17], although they neglected depolarization shift terms, which is a serious handicap for their predictions for wide quantum wells.

In this letter we study the semiconductor Bloch equations without RWA from a nonlinear dynamical systems perspective and find, in qualitative agreement with previous work by Birnir and Galdrikian [2], that for the two-subband driven near resonance period doubling bifurcations or optical bistability may occur. For a three-subband QW designed for this project and driven at resonance $\omega = E_{20}$ several types of bifurcations may occur depending on the shape of the well and the sheet density. We observe a Hopf bifurcation producing a strong signal at a lower frequency than the frequency of the drive. This signal corresponds to a dressing of E_{10} and for a different (lower) value of the field strength a period-doubling bifurcation is observed that also produces a strong signal but now at half the frequency of the drive. Both signals are produced at moderate values of the field strength. The latter result is a big improvement over the result in [2] that was much weaker than the fundamental and occurred at relatively large field strength. Our approach can in principle be applied to any multisubband systems, but in practice when $\omega \geq E_{20}$ one may run in problems such as coupling the system to the continuum or the excitation of LO phonons (if $\omega > 36\text{meV}$). However, these problems can be avoided by introducing more barriers in the well which create several closely spaced subbands as in Figure 1.

The optical properties of the confined electrons in the QW can be studied with the many-body Hamiltonian written in terms of field operators. The electron contribution is given by

$$\begin{aligned} \hat{H}_{el} = & \int d^3x \hat{\psi}^\dagger(x, t) \left(-\frac{1}{2m} \hbar^2 \nabla^2 + W(z) \right) \hat{\psi}(x, t) + \\ & \frac{e^2}{2} \int d^3x \int d^3x' \hat{\psi}^\dagger(x, t) \hat{\psi}^\dagger(x', t) \frac{1}{|x - x'|} \hat{\psi}(x', t) \hat{\psi}(x, t) \\ & - e\mathcal{E}(t) \int d^3x \hat{\psi}^\dagger(x, t) z \hat{\psi}(x, t), \end{aligned} \quad (1)$$

where $W(z)$ is the bare QW potential. It is also assumed that the electric field generated from the radiation off the collective oscillations inside the QW are negligible compared with the laser light \mathcal{E} . The field operators expressed as a linear combination of annihilation operators $a_{k,n}$ are

$$\hat{\psi}(x, t) \equiv \sum_{k,n} \frac{e^{ik \cdot \rho}}{\sqrt{A}} \xi_n(z) a_{k,n}(t)$$

where $\xi_n(z)$ is the self-consistent n-th Hartree eigenstate, k is the in-plane wave vector and A is the QW area. The Hamiltonian can be rewritten in terms of (time-dependent) annihilation and creation operators as

$$\begin{aligned} H = & \sum_k E_n(k) a_{k,n}^\dagger a_{k,n} - \frac{1}{2} \sum_{k,k',\{n\}} V_{\{n\}}^0 a_{k,n}^\dagger a_{k',n_1}^\dagger a_{k',n_2}^\dagger a_{k',n_3} a_{k,n_4} \\ & + \frac{1}{2} \sum_{q \neq 0, k, k', \{n\}} V_{\{n\}}(q) a_{k+q, n_1}^\dagger a_{k'-q, n_2}^\dagger a_{k', n_3} a_{k, n_4} \\ & + \sum_{k, k', n_1, n_2, n} V_{n_1 n n n_2}^0 f_n(k') a_{k, n_1}^\dagger a_{k, n_2} \\ & - \sum_{k, n, m} \mu_{n,m}(k) \mathcal{E}(t) a_{k,n}^\dagger a_{k,m}, \end{aligned} \quad (2)$$

where $E_n(k)$ is the self-consistent Hartree energy, $\mu_{n,m}$ is the dipole moment between the n-th and m-th states, $f_n(k)$ is the Fermi occupation number for the nth-subband and the Coulomb interaction terms are

$$V_{\{n\}}(q) = \frac{2\pi e^2}{\epsilon_0 A} \int dz_1 \int dz_2 \frac{\xi_{n_1}(z_1) \xi_{n_2}(z_2) \xi_{n_3}(z_2) \xi_{n_4}(z_1)}{q} e^{-q|z_1 - z_2|}$$

$$V_{\{n\}}^0 = \frac{2\pi e^2}{\epsilon_0 A} \int dz_1 \int dz_2 \xi_{n_1}(z_1) \xi_{n_2}(z_2) |z_1 - z_2| \xi_{n_3}(z_2) \xi_{n_4}(z_1)$$

where ϵ_0 is the static dielectric constant in GaAs, which is approximately 13. In addition to the usual exchange terms that appear in the electron gas Hamiltonian we obtain depolarization shift terms in the Hamiltonian which are due to the electron shielding and the quasi two-dimensional character of the problem (it is not negligible in wide quantum wells with sheet densities $> 10^{11} e/\text{cm}^2$). The interaction with the laser light is introduced through the electric dipole approximation which implies that any momentum transfer due to the THz radiation is neglected.

Hamiltonian in hand, we proceed with the derivation of the equations of motion for the density matrix in the time-dependent Hartree-Fock approximation, which are also known as the semiconductor Bloch equations. They provide the collective optical response of the electrons to the laser light. In order to be more realistic we introduce dissipation in our equations of motion. Energy (inelastic) and momentum (elastic) scatterings are accounted for albeit phenomenologically (by the relaxation-time approximation).

The dynamics for the density matrix elements $\sigma_{n,n'}(k) = \langle a_{k,n}^\dagger a_{k,n'} \rangle$ are obtained from the Heisenberg equations of motion for the operator $a_{p,n}^\dagger a_{p,n'}$ followed by a quantum statistical average and the Hartree-Fock approximation. We finally obtain, see [8] for details,

$$\begin{aligned} -i\hbar \dot{\sigma}_{n,n'}(k) = & E_{n,n'}(k) \sigma_{n,n'}(k) + i \frac{\hbar}{T_{nn'}} (\sigma_{n,n'}(k) - f_n(k) \delta_{nn'}) \\ & - \sum_{q \neq 0, n_1 n_2 n_3} V_{n_1 n_2 n_3 n}(q) \sigma_{n_1 n_3} (|k - q|) \sigma_{n_2 n'}(k) \\ & + \sum_{q \neq 0, n_2 n_3 n_4} V_{n' n_2 n_3 n_4}(q) \sigma_{nn_3}(k) \sigma_{n_2 n_4} (|k - q|) \\ & - \sum_{k', n_2 n_3 n_4} V_{n' n_2 n_3 n_4}^0 \sigma_{n, n_4}(k) (\sigma_{n_2 n_3}(k') - f_{n_2}(k') \delta_{n_2, n_3}) \\ & - \sum_{k', n_1 n_2 n_3} V_{n_1 n_2 n_3 n}^0 \sigma_{n_1, n'}(k) (\sigma_{n_2 n_3}(k') - f_{n_2}(k') \delta_{n_2, n_3}) \end{aligned}$$

$$+ \sum_m \mathcal{E}(t) (\mu_{mn} \sigma_{mn'}(k) - \mu_{n'm} \sigma_{nm}(k)) \quad (3)$$

where $E_{n,n'}(k) = E_n(k) - E_{n'}(k)$ and $T_{nn'}$ is the experimentally measured relaxation time, see Heymann et al. [3]. Another approximation is to consider the effective masses of all subbands equal, which is fairly accurate for AlGaAs QW's. We also neglect the exchange terms since their inclusion does not modify qualitatively our results and the analysis becomes simpler. It can be shown analytically that this is a good approximation for high sheet densities, since then the kinetic energy terms dominate [18]. With these approximations and a sum over k performed, the dynamics for the averaged density matrix becomes

$$\begin{aligned} -i\hbar \frac{\partial}{\partial t} \sigma_{n,n'} &= (E_n - E_{n'}) \sigma_{n,n'} + i \frac{\hbar}{T_{nn'}} (\sigma_{n,n'} - \sigma_{nn'}^0) \\ + AN_s \sum_{n_2 n_3 n_4} V_{n'n_2 n_3 n_4}^0 \sigma_{n,n_4} (\sigma_{n_2 n_3} - \sigma_{n_2 n_3}^0) \\ - AN_s \sum_{n_1 n_2 n_3} V_{n_1 n_2 n_3 n}^0 \sigma_{n_1, n'} (\sigma_{n_2 n_3} - \sigma_{n_2 n_3}^0) \\ - \sum_m \mathcal{E}(t) (\mu_{mn} \sigma_{mn'} - \mu_{n'm} \sigma_{nm}) \end{aligned} \quad (4)$$

where $\sigma_{n,n'} = \frac{1}{AN_s} \sum_k \sigma_{n,n'}(k)$, N_s is the sheet density and $\sigma_{nn'}^0$ is the equilibrium density matrix. The equations were put in dimensionless form by dividing all terms by E_{20} .

The QW studied was designed to have length 310 Å, depth of 300 meV, two barrier steps of 26 Å in width and 150 meV in height. Figure 1 shows the effective well-shape with a sheet density $N_s = 3.0 \times 10^{11} e/cm^2$. The equations (4) for three subbands only were integrated using the fourth-order Runge-Kutta method with 2048 steps per cycle of drive and the results are plotted in Figures 2-4.

Figure 2 shows the bifurcation diagram of the dipole moment of the collective oscillations. The scaled dipole moment $\langle \mu(t) \rangle / \mu_{10}$ is plotted as a function of the unitless field amplitude $\lambda = e\mathcal{E}z_{10}/E_{20}$. A PDB in the Poincaré map at $\lambda = 0.17$ followed by a Hopf bifurcation (as the field decreases) at $\lambda = 0.378$ are observed. We found an optimum sheet density in which the bifurcations occur with greatest strength and at the same time require small field amplitude, such information can be used as a guide for the experimentalist. For $N_s < 0.5 \times 10^{11} e/cm^2$ and for $N_s > 6.0 \times 10^{11} e/cm^2$ the bifurcations become too small for practical observations. The phase portrait of the Poincaré map in Figure 3 shows the scaled dipole moment plotted against its time derivative (on the vertical axis) for various values of field strength before and after the Hopf bifurcation. This plot is the strongest evidence that Hopf bifurcations occur for our system. Near $\lambda = 0.378$ a supercritical Hopf bifurcation is observed as we decrease the field intensity, the fixed point, a periodic orbit with the frequency of the drive, becomes unstable

generating a small closed orbit. Several of those orbits are plotted each one corresponding to a fixed value of the field strength, decreasing the field amplitude gives a new and larger closed orbit.

The period-doubling can be understood as a two-photon process, see [2], its increased strength in this letter is due to the fact that it is being assisted by the presence of almost equally spaced (in frequency) frequencies E_{10} and E_{20} . The dynamics of the electron gas correspond to a periodic orbit of twice the period of the response before the bifurcation.

The large and broad peak at roughly $\omega/2$ is the main feature of the bifurcation as can be seen in Figure 4 which shows the power spectrum before and after the Hopf bifurcation. The peak in Figure 4 is broad due to the difference frequencies, dressed $\pm(E_{21} - E_{10})$, that are clearly visible on each side of the incommensurate peak. The half-frequency peaks (not shown) for the PDB are sharp in distinction [2]. By varying the sheet density and field strength the incommensurate peak can be tuned but this will be explored in Batista, Tamborenea and Birnir [8]. In Figure 4 we also observe a DC response that coincides with the frequency axis. The dynamics of the electron gas after (decreasing λ) the Hopf bifurcation corresponds to a quasi periodic orbit on a torus defined by the incommensurate frequency and the fundamental. At both the PDB and Hopf bifurcations the populations of the upper subbands are suddenly increased at the expense of the zeroth subband. The frequency of the drive is of the order of 20 meV, which is in the range of the FEL (however, E_{20} can be lowered by decreasing the tunneling if necessary).

The realization that QWs can undergo a Hopf bifurcation (from a periodic orbit) only observed before in classical nonlinear systems can lead to many applications including frequency down-converters. In our QW the lower subbands are almost equally spaced, but that could be easily changed by increasing its asymmetry and eventually eliminating the possibility of PDBs. The asymmetry though cannot be too big otherwise the tunnelling is reduced and we cannot guarantee that our three-subband system driven at resonance with E_{20} is really isolated from upper subbands and the continuum.

The authors would like to thank Mark Sherwin, S. James Allen and Atac Imamoglu for helpful comments and discussions. The idea of nonlinear bifurcations in quantum wells were inspired by J. D. Crawford's elegant exposition on bifurcation theory [19]. The work was supported by NSF grants DMS-9704874, DMS-0072191 and a DARPA-Navy grant N00014-99-10935.

- [1] J. N. Heyman *et al.*, Phys. Rev. Lett. **72**, 2183 (1994).
- [2] B. Galdrikian and B. Birnir, Phys. Rev. Lett. **76**, 3308 (1996).
- [3] J. N. Heyman *et al.*, Phys. Rev. Lett. **74**, 2682 (1995).
- [4] K. Craig *et al.*, Phys. Rev. Lett. **76**, 2382 (1996).
- [5] M. Zaluźny, Phys. Rev. B **47**, 3995 (1993).
- [6] M. Zaluźny, J. Appl. Phys. **74**, 4716 (1993).
- [7] The Hopf bifurcation is well known to be related to the Ruelle-Takens quasi-periodic route to chaos in classical systems [19].
- [8] A. A. Batista, P. I. Tamborenea and B. Birnir (2001), to be published.
- [9] A. A. Batista, B. Birnir and M. S. Sherwin, Phys. Rev. B **61**, 15108 (2000).
- [10] M. S. Sherwin *et al.*, Physica D **83**, 229 (1995).
- [11] M. S. Sherwin, Current Opinion in Solid State and Materials Science **3**, 191 (1998).
- [12] H. Haug and S. W. Koch, *Quantum Theory of the optical and electronic properties of semiconductors* (World Scientific, Singapore, 1990).
- [13] S. L. Chuang, M. S. C. Luo, S. Shmitt-Rink and A. Pinczuk, Phys. Rev. B **46**, 1897 (1992).
- [14] M. S-C. Luo, S. L. Chuang, S. Schmitt-Rink and A. Pinczuk, Phys. Rev. B **48**, 11086 (1993).
- [15] D. E. Nikonov, A. Imamoglu, L. V. Butov and H. Schmidt, Phys. Rev. Lett. **79**, 4633 (1997).
- [16] D. E. Nikonov, A. Imamoglu and M. O. Scully, Phys. Rev. B **59**, 12212 (1999).
- [17] L. Tsang, C. Chansungsan and S. L. Chuang, Phys. Rev. B **45**, 11918 (1992).
- [18] A. L. Fetter and J. Walecka, *Quantum theory of many-particle systems* (McGraw-Hill, San Francisco, 1971).
- [19] J. D. Crawford, Rev. of Mod. Phys. **63**, 991 (1991).

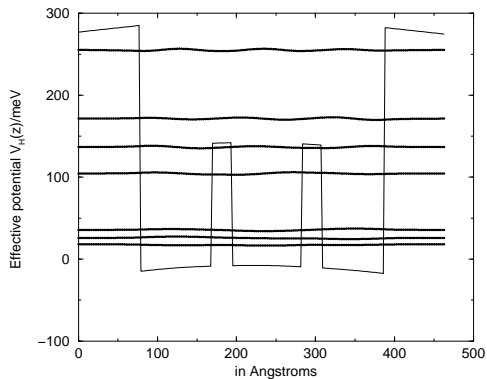


FIG. 1. The stationary self-consistent potential for a sheet density of $N_s = 3.0 \times 10^{11} e/cm^2$, and its first seven eigenstates with asymptotes set to their energies. The double barrier creates, through tunneling, three closely spaced subbands well isolated from upper subbands. The slight asymmetry enhances the nonlinear effects, but too much asymmetry reduces the tunneling and with it the decoupling with upper subbands.

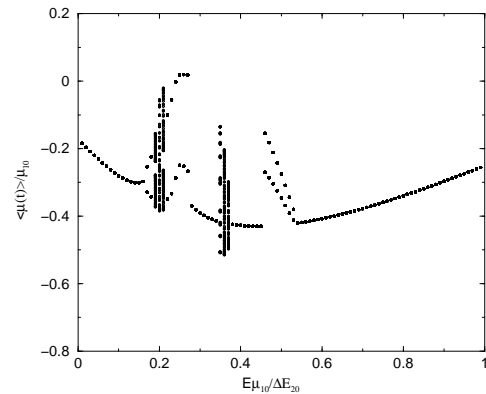


FIG. 2. The Poincaré map of the averaged dipole moment in the doped QW with a sheet density of $N_s = 3.0 \times 10^{11} e/cm^2$. With increasing field strength a PDB occurs at $\lambda = 0.17$. At $\lambda = 0.378$ a supercritical Hopf bifurcation occurs, as the field is decreased below this value. The two branches of the PDB undergo a Hopf bifurcation at $\lambda = 0.19$.

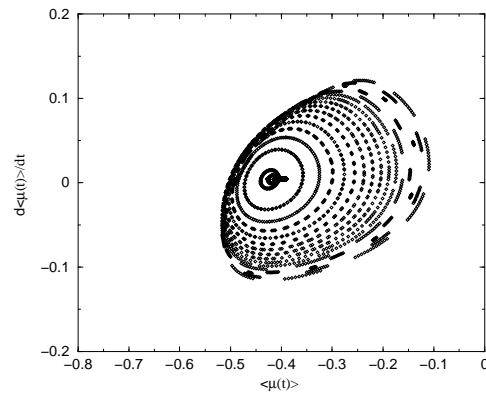


FIG. 3. Phase portrait view of the Hopf bifurcation in the quantum well. Each one of the closed orbits corresponds to a different value of the field amplitude, with $\lambda = 0.34 - 0.38$ and a sheet density of $N_s = 3.0 \times 10^{11} e/cm^2$.

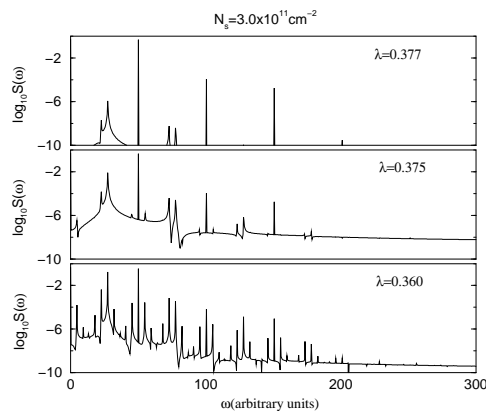


FIG. 4. Power spectra of the dipole moment for the doped asymmetric quantum well near the onset of the supercritical Hopf bifurcation. As we decrease the field past $\lambda = 0.38$ the low frequency signal grows continuously. The zero frequency peak coincides with the y-axis and extends to zero.